Proc. Natl. Acad. Sci. USA
Vol. 86, pp. 607–611, January 1989
Immunology

Three-dimensional structure of Fab R19.9, a monoclonal murine antibody specific for the *p*-azobenzenearsonate group

M.-B. LASCOMBE*, P. M. ALZARI*, G. BOULOT*, P. SALUDJIAN*, P. TOUGARD*, C. BEREK†, S. HABA‡, E. M. ROSEN‡, A. NISONOFF‡, AND R. J. POLJAK*§

*Département d'Immunologie, Institut Pasteur, 75015 Paris, France; †Institute of Genetics, University of Cologne, Cologne 41, Federal Republic of Germany; and ‡Rosenstiel Research Center, Department of Biology, Brandeis University, Waltham, MA 02254

Contributed by A. Nisonoff, August 8, 1988

ABSTRACT **The crystal structure of Fab R19.9, derived from an anti-*p*-azobenzenearsonate monoclonal antibody, has been determined and refined to 2.8-Å resolution by x-ray crystallographic techniques. Monoclonal antibody R19.9 (IgG2bκ) shares some idiotopes with a major idiotype (CRI_A) associated with A/J anti-*p*-azobenzenearsonate antibodies. The amino acid sequences of the variable (V) parts of the heavy (V_H) and light (V_L) polypeptide chains of monoclonal antibody R19.9 were determined through nucleotide sequencing of their mRNAs. The V_L region is very similar to that of CRI_A-positive anti-*p*-azobenzenearsonate antibodies as is V_H, except for its third complementarity-determining region, which is three amino acids longer; it makes a loop, unique to R19.9, that protrudes into the solvent. A large number of tyrosine residues in the complementarity-determining region of V_H and V_L, with their side chains pointing towards the solvent, may have an important function in antigen binding.**

Murine antibodies to model antigens have provided valuable experimental systems to study the molecular bases of the specificity, diversity, and genetic control of immune responses. The hapten, *p*-azobenzenearsonate (Ar), has been used in several laboratories as a suitable probe for such studies (1–5), which have been facilitated by the presence of an intrastrain cross-reactive idiotype, designated CRI_A, among the anti-Ar antibodies of A/J mice or of closely related strains. The expression of CRI_A is linked to genetic loci encoding heavy (H) chains (6) and light (L) chains (7). On the average, about half of the anti-Ar antibodies induced by keyhole limpet hemocyanin-Ar in A/J mice share this idiotype. The variable (V) regions, V_H and V_L, of CRI_A^+ antibodies appear to be encoded by single germ-line genes (8, 9), and the diversity (D) region is encoded by a variant of the DFL16.1 gene (10). CRI_A^+ molecules also utilize the $V_\kappa 10$, κ chain joining (J) 1, and, almost invariably, $J_H 2$ gene segments (4, 5, 11). Idiotype-expressing antibodies from hyperimmunized mice display somatic variants of amino acid sequences in each of these gene segments (4, 5, 12), whereas the antibodies from an early primary response reflect few if any mutations (5). The V_H region appears to be somewhat more susceptible to somatic variation than V_L (4). A disproportionate number of mutations in V_H and V_L occurs in their complementarity-determining regions (CDR); this probably reflects selection by antigen of variants with higher affinity (5).

Among the serum anti-Ar antibodies of immunized A/J mice are molecules that carry some but not all of the idiotopes associated with CRI_A (13, 14). Such antibodies are bound by anti-CRI_A antibodies, but they are unable to completely displace labeled CRI_A^+ antibodies from such anti-idiotype antibodies. Antibodies of this type were designated "minor idiotypes" (13, 14). The subject of the present investigation, monoclonal antibody (mAb) R19.9 (IgG2bκ), has these serological properties and is thus a member of a minor idiotypic anti-Ar family. The L chains of R19.9, when combined with H chains of a CRI_A^+ mAb, yielded a CRI_A^+ product (14). However, the converse recombinant ($H_{19.9}L_{CRI}$) was CRI_A^- by the criterion of inhibition in the standard assay for CRI_A. Amino acid sequences (this paper) indicate that the $V_\kappa 10$, $J_\kappa 1$, V_H, and $J_H 2$ sequences of R19.9 are closely related to the putative germ-line sequences controlling CRI_A but that the D_H sequence (in CDR3 of V_H) differs markedly; it is 3 residues longer than the characteristic D_H sequence (11 vs. 8 residues). There are also three amino acid substitutions in CDR2 of V_H that may contribute to the idiotypic variance of R19.9.

The x-ray crystallographic study of Fab R19.9 presented here permits a correlation between amino acid sequences, idiotypic markers, and the three-dimensional structure of the A/J anti-Ar antibodies. Tentative conclusions can also be drawn about the conformation of the antigen-combining site of anti-Ar molecules.

MATERIALS AND METHODS

The monoclonal, A/J anti-Ar antibody R19.9 (IgG2bκ) was prepared as described (15, 16). After papain digestion (17), the Fab fragment of R19.9 was extensively purified by three successive column chromatography steps with Sephadex G-100 (Pharmacia), DEAE-cellulose (0.76 milliequivalent per g; Serva, Heidelberg) equilibrated in 0.04 M potassium phosphate buffer, and PBE 94 (Pharmacia) for chromatofocusing. In this last step, the Fab was eluted with Polybuffer 96 (Pharmacia) as a major peak at pH 7.5–7.6. The purified Fab of R19.9 was crystallized at room temperature by vapor diffusion in hanging drops (18) or in capillaries against 20% (wt/vol) PEG 8000 (Sigma)/0.2 M sodium chloride/3 mM sodium azide/0.1 M potassium phosphate, pH 7.3 (19). The crystals grow to a size of up to 0.3 mm × 0.4 mm × 1.5 mm. They are monoclinic, space group $P2_1$, with unit cell dimensions $a = 43.3$ Å, $b = 80.8$ Å, $c = 75.1$ Å, $\beta = 96°$. There is one Fab in the asymmetric unit.

X-ray intensity data were measured on a diffractometer with CuKα radiation. Since the crystals of Fab R19.9 are polymorphic (19), they were carefully selected to conform to the unit cell dimensions given above. Crystals were replaced with the intensities of reference reflections decreased below 70% of their starting values. Integrated intensities were obtained by profile fitting (20) and were further corrected for Lorentz-polarization factors, absorption (21), and radiation decay. For the native crystals, a complete data set to 2.8-Å

Abbreviations: Ar, *p*-azobenzenearsonate; CRI_A, major cross-reactive idiotype associated with anti-Ar antibodies of the A strain of mouse; H, heavy; L, light; V, variable; D, diversity; J, joining; C,

Table 1. Crystallographic refinement of Fab R19.9

Parameter	Actual rms deviation, Å	Target σ
Deviation from ideal distances		
Bond distances	0.011	0.020
Angle distances	0.091	0.060
Planar 1-4 distances	0.085	0.060
Deviation from planarity	0.006	0.020
Deviation from permitted constant distances		
Single torsion contacts	0.349	0.500
Multiple torsion contacts	0.465	0.500
Possible hydrogen bond	0.469	0.500

R factor $= \sum_h \sum_k \sum_l ||F_{obs}| - |F_{calc}|| / \sum_h \sum_k \sum_l |F_{obs}| = 0.296$; number of structure factors $F > 2\sigma = 12{,}145$.

resolution was obtained from 26,284 measurements that were merged to yield the intensities of 13,138 independent reflections ($R_{sym} = 0.074$). Three heavy atom derivatives were obtained by using phenylmercury(II) acetate, *p*-hydroxymethylbenzenesulfonate, and $OsCl_6$. Their intensities were measured to 3.5-Å [phenylmercury(II) acetate and *p*-hydroxymethylbenzenesulfonate] and 6-Å ($OsCl_6$) resolution. After refinement of heavy atom occupancies, scale factors, and thermal (isotropic) and positional parameters, an electron density map was calculated to 3.5-Å resolution (average figure of merit, $m = 0.52$). The interpretation of this map was facilitated by a six-dimensional real space search by using the model of Fab New (22) as a search object. A rotation function calculation (23) gave a clear indication of the orientation of the Fab in the unit cell, in agreement with that found by the model search of the electron density map. The positions of the V_H, V_L, C_H1, and C_L domains were refined at 6-Å resolution by a constrained-restrained least-squares procedure [CORELS (24)]. At this stage the agreement factor, R, between observed (obs) and calculated (calc) structure factors (F), $R = \Sigma(F_{obs} - F_{calc})/\Sigma(F_{obs})$, was 42%. A solvent-flattened (25) electron density map at 3.5-Å resolution ($m = 0.81$, $\Delta\phi = 35°$) allowed the tracing of most of the polypeptide chain. The amino acid sequence of Fab R19.9 was adjusted to the electron density map using the program FRODO (26) on a PS300 Evans and Sutherland interactive graphics system. The model was refined by the restrained least-squares program PROLSQ (27) by using reflections between 10- and 2.8-Å resolution. After 33 cycles of refinement ($R = 32.4\%$), the model was partially rebuilt based on difference Fourier ($2F_{calc} - F_{obs}$, α_{calc}) and "OMIT" (28) maps, as well as inspection of the solvent-flattened electron density map. The structure was further improved by alternating model building on difference Fourier and OMIT maps followed by PROLSQ refinement until reasonable convergence was achieved (see Table 1). The current R factor is 0.296. No attempt was made to place solvent molecules in the model.

Sequencing of polysomal mRNA for V_H and V_κ was carried out according to Griffiths and Milstein (29) by using primers described previously (30, 31).

RESULTS

The 3.5-Å resolution electron density map described above was used to fit the amino acid sequences of the variable regions [V_H, D, and J_H2 and also V_κ and J_κ (see Figs. 1 and 2)] and those of the constant regions, C_H1 of IgG2b and C_κ (32). Since the sequence of V_H was determined for residues 16–123 only, the first 15 residues were assumed to be the same as those in protein 36-65, which expresses the germ-line-encoded V_H sequence of CRI_A (8). This choice seemed reasonable because the same V_H germ-line gene is expressed in 36-65 and R19.9 and because in 11 published N-terminal sequences of CRI_A^+ mAbs there is a total of only seven amino acid substitutions in this region (33, 34). Although the electron density maps gave an indication for the trace of the polypeptide chain in CDR3 of V_H, the detailed conformation of this region was less clear than that of other parts of Fab R19.9. V_H positions 34, 55, 58, 59, and 74 differ from those of the germ-line V_H gene; however, the electron density map showed good agreement with the experimentally determined V_H sequence (Fig. 1) at those positions. Although the ambiguity (His/Asp) at V_H position 105 cannot be resolved with certainty by the electron density map, aspartic acid

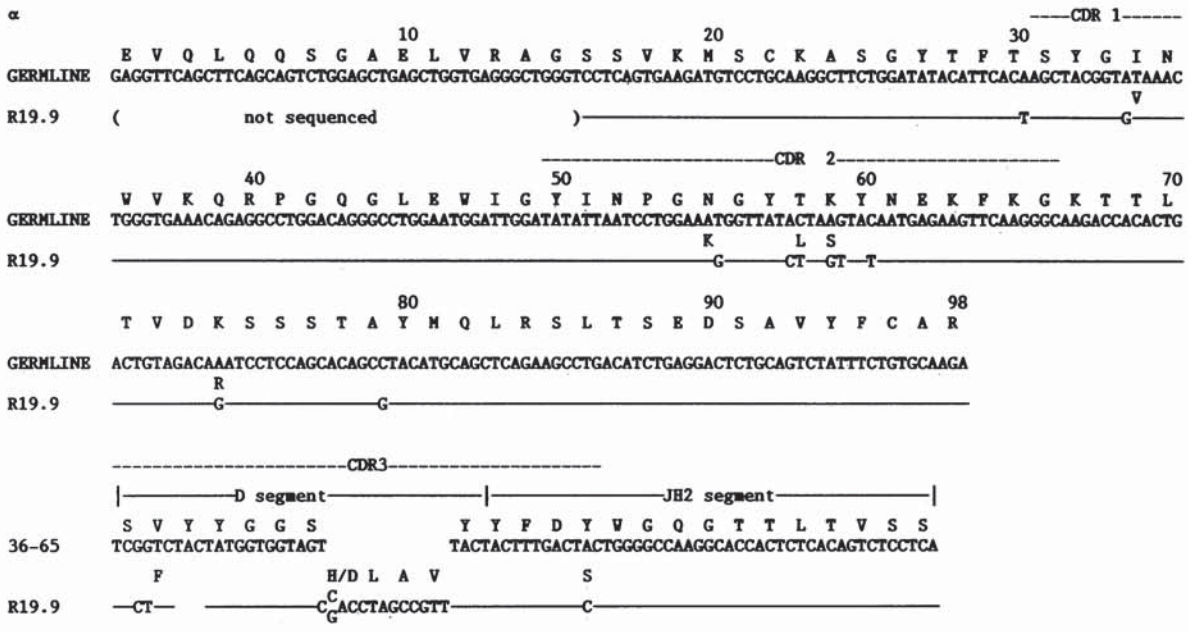

FIG. 1. Nucleotide and deduced amino acid sequences of the V_H region of mAb R19.9. They are compared, between residues 1–98, with

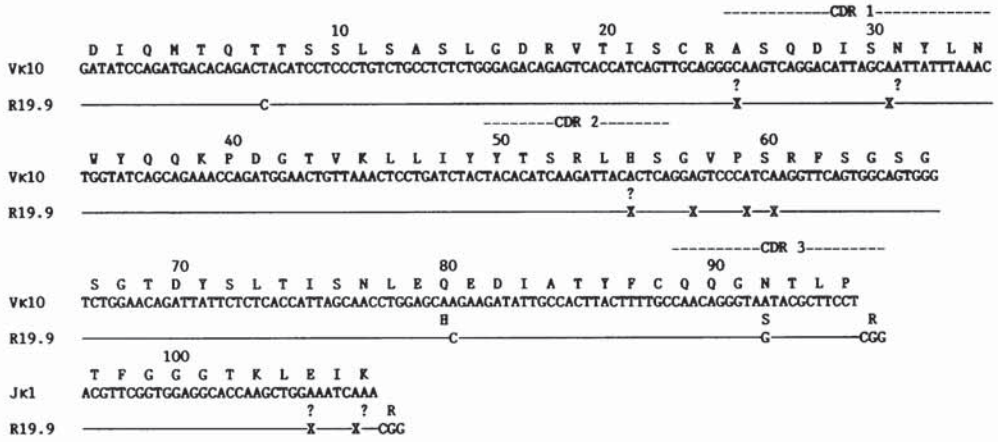

FIG. 2. Nucleotide and deduced amino acid sequences of the V_κ region of mAb R19.9. Comparison is made with sequences of the V_κ10-Ars-A and J_κ1 genes that encode CRI_A^+ mAb (9). See legend to Fig. 1. ?, undetermined nucleotide.

seems to be the best choice. Electron density features in V_L positions 31, 55, and 107 correspond reasonably well with the amino acid sequence encoded by the V_κ10-Ars-A germ-line gene that encodes the V_L region of CRI_A^+ antibodies and to the J_κ1 germ-line sequence (Fig. 2). At position 105, where an ambiguity in the nucleotide sequence is consistent with the presence of alanine, glutamic acid, glycine, or valine, the electron density map favors glutamic acid, in agreement with the germ-line J_κ1 sequence.

The domain structure of Fab R19.9 closely follows that observed for all Fabs whose three-dimensional structure has been determined by x-ray diffraction to date (reviewed in refs. 35 and 36). The quaternary structure of Fab R19.9 is that of an extended conformation. This conformation is usually described by reference to an "elbow" angle made by the pseudo 2-fold axes relating V_H to V_L and C_H1 to C_L. For Fab R19.9 this angle is 178°, which is the largest (closest to 180°) so far observed in Fab structures. The rotation-translation operations necessary to superimpose selected α-carbon backbones of V_H and V_L are 175° and 0.45 Å, respectively, indicating a nearly ideal symmetry relationship between those domains. The numerical values for the corresponding operations in the C_H1–C_L domains are 168° and 1.5 Å, values similar to those of other known Fab structures.

A measure of the closeness of the Fab R19.9 structure to that of several other Fab molecules can be obtained by analyzing the shifts in the relative positions of packed β-sheets (37). Thus, if the spatial superposition of the V_H or V_L β1 sheets is optimized, the β2 sheets of different Fabs (listed in Table 2) are no further away than an average of 0.55 Å and a rotation angle of 9° from the corresponding sheet of Fab R19.9.

The relative disposition of V_H and V_L in Fab R19.9 can be further compared to those of other Fabs by superposing the α-carbon coordinates of the residues that define the interface between the V_H and V_L subunits, as described in Table 2. The largest deviations that were observed for Fab R19.9 are 1.5 Å and 12.8°. These deviations and others observed with different Fabs do not appear to be significant.

DISCUSSION

The three-dimensional structure of Fab R19.9 presented here provides a structural model of a specific hapten-binding mAb of predefined specificity. The calculation of electron density maps at 2.8-Å resolution by x-ray crystallographic techniques and the determination of amino acid sequences (through nucleotide sequencing of the mRNAs) of V_H and V_L allowed in the different electron density maps that were calculated, its side chains could not be placed unambiguously. The ambiguity may arise from an intrinsic high mobility of V_H CDR3. This possibility is supported by the fact that the long V_H CDR3 loop protrudes into the solvent beyond other parts of the molecule (see Fig. 3).

The three-dimensional structure of Fab R19.9 agrees well with those of other Fabs that have been determined. It displays the largest elbow angle that has been observed in Fabs, in agreement with the idea that an extended (or contracted) conformation is independent of ligand binding to the combining site. As shown in Table 2, the relative disposition of V_H and V_L in Fab R19.9 is well within a spectrum of angular and translational values observed in a number of Fabs, irrespective of their human or murine origin or of their liganded or unliganded state. The difference in relative disposition of V_H and V_L observed by Colman *et al.* (45) in a neuraminidase complex falls in the range of those observed in Table 2, indicating that formation of a complex with

Table 2. The relative arrangements of V_H and V_L domains in different Fabs

	Hy5	Kol	New	J539	McPC603	R19.9	D1.3
Hy5		0.49 Å 0.54 Å	0.70 Å 0.69 Å	0.42 Å 0.67 Å	0.53 Å 0.39 Å	0.68 Å 0.95 Å	0.69 Å 0.62 Å
Kol	0.96 Å 8.5°		0.78 Å 0.56 Å	0.61 Å 0.49 Å	0.56 Å 0.30 Å	0.74 Å 0.92 Å	0.73 Å 0.55 Å
New	1.14 Å 5.0°	0.36 Å 3.6°		0.64 Å 0.57 Å	0.80 Å 0.62 Å	0.82 Å 0.92 Å	0.87 Å 0.56 Å
J539	0.70 Å 11.0°	1.14 Å 4.5°	1.14 Å 6.7°		0.62 Å 0.54 Å	0.75 Å 1.03 Å	0.77 Å 0.64 Å
McPC603	0.68 Å 4.9°	0.74 Å 5.4°	0.72 Å 3.8°	0.44 Å 7.2°		0.71 Å 0.88 Å	0.57 Å 0.59 Å
R19.9	1.93 Å 6.9°	1.19 Å 9.1°	1.08 Å 8.0°	2.13 Å 12.8°	1.69 Å 6.9°		0.69 Å 0.93 Å
D1.3	0.91 Å 6.8°	0.53 Å 2.6°	0.38 Å 1.9°	0.90 Å 5.1°	0.46 Å 4.8°	1.22 Å 9.5°	

Atomic coordinates for Fab Kol (38), New (22), McPC603 (39), J539 (40), and Hy5 (41) were obtained from the Brookhaven Data Bank (42, 43), and those of Fab D1.3 (44) were obtained from the authors. The V_L domain of the Fab corresponding to each horizontal row was mapped into the V_L of the Fab in the column by using α-carbon coordinates of residues defining the interface between V_H and V_L domains (45). The calculated transformation was applied to the Fab corresponding to the horizontal row, and the additional translation (Å) and rotation (°) to optimize overlap between the corresponding pair of V_H domains are given in the lower left triangle.

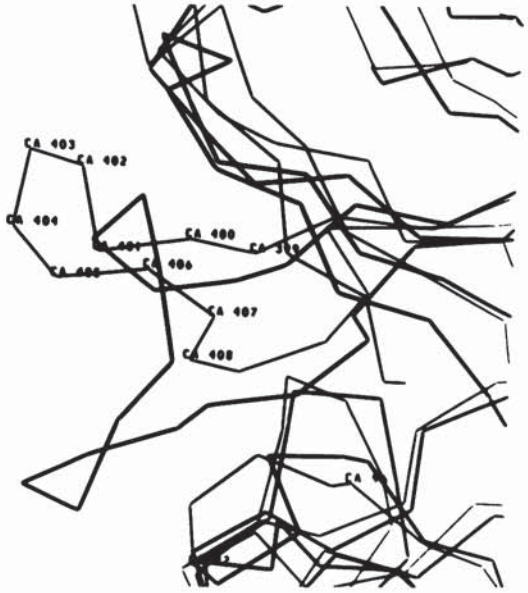

FIG. 3. A superposition of a portion of the α-carbon backbones of Fabs Kol (38) and R19.9. The V_H CDR3 of the Fabs have very different conformations. That of R19.9 is labeled and indicated by a slightly thinner trace. The numbers above 300 represent position numbers in the V_H sequence of R19.9 plus 300.

antigen is not necessary to produce the observed variability in the relative disposition of V_H and V_L.

The CDRs of R19.9 contain a striking number of aromatic side chains, mostly tyrosines, which are oriented in such a way that they expose their phenolic OH groups to the solvent (see Fig. 4). These include the V_H tyrosines 27, 32, 57, 101, and 109. V_H Phe-100 in this region is also exposed to the solvent. V_H Phe-29, Tyr-50, and Tyr-110 are oriented towards the interior of the structure, thus precluding their participation in contacts with ligands. In V_L, Tyr-32, Tyr-49, and Tyr-50 are oriented with their side chains pointing towards the solvent. Thus, a total of nine aromatic side chains belonging to the V_H and V_L CDRs, mostly tyrosines, are positioned to provide possible contacts with antigen. The prevalence of tyrosine residues in these CDRs has been noted

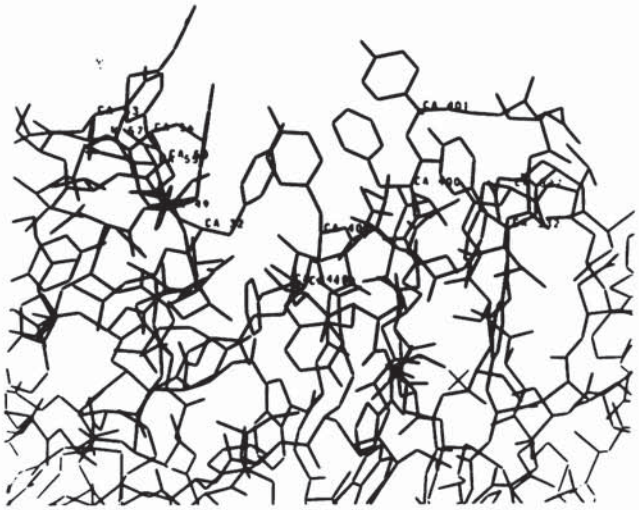

FIG. 4. A view of the combining site of Fab R19.9, which shows a high density of aromatic residues, mostly tyrosine V_L is at left; V_H

by Jeske *et al.* (46), although orientations of these residues were not known.

Site-directed mutagenesis (47) and chain recombination studies (48) have implicated V_H Ser-99 and V_L Arg-96, respectively, as residues that are important in Ar binding. Inspection of the model of Fab R19.9 shows that the guanidino group of V_L Arg-96 is at the bottom of the narrow cavity between V_H and V_L and that it could participate in direct contacts with an Ar ligand. Thus, it provides a positively charged group that could neutralize the negative charge of the Ar hapten. Ser-99 in V_H appears less accessible to interactions with an external ligand. However, it and Arg-96 may be important in hapten binding not only because they could contribute direct contacts with Ar but also through stabilizing interactions with other amino acid residues at the combining site of the antibody itself. A precise identification of residues contacting bound Ar will require the determination of the three-dimensional structure of a hapten–Fab complex.

The presence of a long V_H CDR3 loop in R19.9 has two major effects on the structure of the combining site: (*i*) it partially fills what otherwise would be a large cavity or depression surrounded by the other CDRs of V_H and V_L; and (*ii*) it provides a protruding structural feature that appears unique to R19.9 among other Fab structures that have been determined. It is interesting to compare this loop with that of human V_H KOL (38). Although KOL's CDR3 is three amino acids longer, it is partially bent inwards, thus resulting in a less salient loop than that of R19.9 (Fig. 4).

The anti-Ar mAb R19.9 expresses some but not all idiotopes associated with CRI_A. The nucleotide and amino acid sequences of its V_H and V_κ regions are consistent with the possibility that they are somatic variants of the germ-line V_H and V_κ genes that encode CRI_A antibodies (Figs. 1 and 2). In addition, R19.9 utilizes the canonical J_H2 of CRI_A. A major distinction in R19.9 is the contribution of a D gene segment giving rise to an atypical CDR3 that contains three more amino acid residues than are present in mAbs that fully express CRI_A. The typical eight-residue D sequence appears to arise from the DFL16.1 genetic segment (10). The unusual, longer D segment as well as the three amino acid substitutions in V_H CDR2 are likely to account for the incomplete expression of CRI_A idiotopes in R19.9. In agreement with this conclusion, the L chain of R19.9, when combined with the H chain of a CRI_A^+ mAb, yields a recombinant molecule that expresses CRI_A, whereas the converse recombinant, $H_{R19.9}L_{CRI}$ is idiotypically inactive (14).

The partial idiotypic cross-reactivity between R19.9 and CRI_A^+ mAbs can be explained by the presence, in anti-idiotype sera, of antibodies that recognize residues in V_H and V_L other than those in V_H CDR3. Small differences in the primary structure of R19.9 and the germ-line-encoded structure owing to somatic mutations, as well as the large difference in D-region structure, could also contribute to the lack of total identity in serological tests. Among the somatic variations, the change from Ile-34 to Val in V_H R19.9 does not seem adequate to explain a change in antigenic properties since the amino acid side chain at that position is not exposed. The sequence variations observed at positions Lys-55, Tyr-57, Leu-58, and Ser-59 in CDR2 and Arg-74 in FR3 could readily affect recognition of idiotopes since they are exposed at the accessible surface of V_H.

Characterization of two antigenic determinants occurring on a native protein (41, 44) indicates that the antigen–antibody interface extends over an area of about 700 $Å^2$ and includes residues from each of the V_H and V_L CDRs. Contacts with an anti-idiotype antibody might similarly include residues from all CDRs. Thus, given the solvent-exposed location and the spatial proximity of the CDR loops

Note Added in Proof. After this paper was submitted for publication, Stevens *et al.* (49) reported differences in low and high ionic strength crystalline forms of human immunoglobulin L-chain dimer Loc, which they take to indicate different potential conformations of an antibody. The different V_L–V_L contacts observed in Loc, as well as those between V_H and V_L domains in FabNC41 complexed to antigen (45), are postulated (49) to increase antigenic and idiotypic specificities of antibodies. However, as shown in Table 2, the V_H–V_L contacts observed in NC41 are within the range observed in Fabs, independently of their liganded (D1.3 and Hy5) or nonliganded states. Since Table 2 includes Fabs crystallized at low (Hy5, D1.3, and R19.9) and high ionic strength (Kol, New, J539, and McPC603), the conformational variations observed in Loc may be unique to it or to L chains, which do not normally occur as dimers in nature. The lack of significant differences in the relative disposition of V_H and V_L thus far observed in liganded or unliganded Fabs does not seem to suggest that such differences could contribute to increase the functional diversity of antibodies.

We wish to thank Dr. Claude Riche (Centre National de la Recherche Scientifique, Gif sur Yvette, France) for the interpretation of the electron density map of R19.9 at 6-Å resolution by means of a six-dimensional real space search. This work was supported by grants from the Institut Pasteur, Centre National de la Recherche Scientifique, contract BAP-0221(DC) from the European Economic Community, and by National Institutes of Health grants AI-25369 and AI-22068.

1. Kuettner, M. G., Wang, A. L. & Nisonoff, A. (1972) *J. Exp. Med.* **135,** 579–595.
2. Nisonoff, A., Ju, S.-T. & Owen, F. L. (1977) *Immunol. Rev.* **34,** 89–118.
3. Greene, M. I., Nelles, M. J., Sy, M.-S. & Nisonoff, A. (1982) *Adv. Immunol.* **32,** 253–300.
4. Rathbun, G., Sanz, I., Meek, K., Tucker, P. & Capra, J. D. (1988) *Adv. Immunol.* **42,** 95–164.
5. Manser, T., Wysocki, L. J., Margolies, M. N. & Gefter, M. L. (1987) *Immunol. Rev.* **96,** 141–162.
6. Pawlak, L. L., Mushinski, E. B., Nisonoff, A. & Potter, M. (1973) *J. Exp. Med.* **137,** 22–31.
7. Laskin, J. A., Gray, A., Nisonoff, A., Klinman, N. R. & Gottlieb, P. G. (1977) *Proc. Natl. Acad. Sci. USA* **74,** 4600–4604.
8. Siekevitz, M., Huang, S.-Y. & Gefter, M. L. (1983) *Eur. J. Immunol.* **13,** 123–132.
9. Sanz, I. & Capra, J. D. (1987) *Proc. Natl. Acad. Sci. USA* **84,** 1085–1089.
10. Landolfi, N. F., Capra, J. D. & Tucker, P. W. (1986) *J. Immunol.* **137,** 362–365.
11. Meek, K., Sanz, I., Rathbun, G., Nisonoff, A. & Capra, J. D. (1987) *Proc. Natl. Acad. Sci. USA* **84,** 6244–6248.
12. Estess, P., Lamoyi, E., Nisonoff, A. & Capra, J. D. (1980) *J. Exp. Med.* **151,** 863–875.
13. Gill-Pazaris, L. A., Brown, A. R. & Nisonoff, A. (1979) *Ann. Immunol. (Paris)* **130C,** 199–213.
14. Gill-Pazaris, L. A., Lamoyi, E., Brown, A. R. & Nisonoff, A. (1981) *J. Immunol.* **126,** 75–79.
15. Lamoyi, E., Estess, P., Capra, J. D. & Nisonoff, A. (1980) *J. Immunol.* **124,** 2834–2840.
16. Amit, A. G., Harper, M., Mariuzza, R. A., Saludjian, P., Poljak, R. J., Lamoyi, E. & Nisonoff, A. (1983) *J. Mol. Biol.* **165,** 415–417.
17. Porter, R. R. (1959) *Biochem. J.* **73,** 119–127.
18. Wlodawer, A. & Hodgson, K. O. (1975) *Proc. Natl. Acad. Sci. USA* **72,** 398–399.
19. Mariuzza, R. A., Amit, A. G., Boulot, G., Saludjian, P., Saul, F., Tougard, P., Poljak, R. J., Conger, J., Lamoyi, E. & Nisonoff, A. (1984) *J. Biol. Chem.* **259,** 5954–5958.
20. Oatley, S. & French, S. (1982) *Acta Crystallogr. Sect. A* **38,** 537–549.
21. North, A. C. T., Phillips, D. C. & Matthews, F. S. (1968) *Acta Crystallogr. Sect. A* **24,** 351–358.
22. Saul, F. A., Amzel, L. M. & Poljak, R. J. (1978) *J. Biol. Chem.* **253,** 585–597.
23. Crowther, R. A. (1972) *The Molecular Replacement Method*, ed. Rossmann, M. G. (Gordon & Breach, New York), pp. 173–178.
24. Sussman, J. L. (1985) *Methods Enzymol.* **115,** 271–303.
25. Wang, B. C. (1985) *Methods Enzymol.* **115,** 90–122.
26. Jones, T. A. (1985) *Methods Enzymol.* **115,** 157–171.
27. Hendrickson, W. A. & Konnert, J. H. (1980) in *Computing in Crystallography*, eds. Diamond, R., Ramaseshan, S. & Venkatesan, K. (Indian Acad. Sci., Bangalore, India), pp. 13.01–13.25.
28. Bhat, T. N. (1988) *J. Appl. Crystallogr.* **21,** 279–281.
29. Griffiths, G. M. & Milstein, C. (1985) in *Hybridoma Technology in Biosciences and Medicine*, ed. Springer, T. A. (Plenum, New York), pp. 103–115.
30. Kaartinen, M., Griffiths, G. M. & Milstein, C. (1983) *Nature (London)* **304,** 320–324.
31. Robbins, P. F., Rosen, E. M., Haba, S. & Nisonoff, A. (1986) *Proc. Natl. Acad. Sci. USA* **83,** 1050–1054.
32. Kabat, E. A., Wu, T. T., Reid-Miller, M., Perry, H. M. & Gottesman, K. S. (1987) *Sequences of Proteins of Immunological Interest* (U.S. Public Health Service, National Institutes of Health, Bethesda, MD), 4th Ed.
33. Slaughter, C. A. & Capra, J. D. (1984) in *Biology of Idiotypes*, eds. Greene, M. I. & Nisonoff, A. (Plenum, New York), pp. 35–58.
34. Huang, S. Y., Margolies, M. N., Marshak-Rothstein, A., Siekevitz, M. & Gefter, M. L. (1982) *Pharmacol. Rev.* **34,** 43–49.
35. Davies, D. R. & Metzger, H. A. (1983) *Annu. Rev. Immunol.* **1,** 87–117.
36. Alzari, P. M., Lascombe, M.-B. & Poljak, R. J. (1988) *Annu. Rev. Immunol.* **6,** 555–580.
37. Lesk, A. M. & Chothia, C. (1982) *J. Mol. Biol.* **160,** 325–342.
38. Marquart, M., Deisenhofer, J., Huber, R. & Palm, W. (1980) *J. Mol. Biol.* **141,** 369–391.
39. Satow, Y., Cohen, G. H., Padlan, E. A. & Davies, D. R. (1986) *J. Mol. Biol.* **190,** 593–604.
40. Suh, S. W., Bhat, T. N., Navia, M. A., Cohen, G. H., Rao, D. N., Rudikoff, S. & Davies, D. R. (1986) *Proteins* **1,** 74–80.
41. Sheriff, S., Silverton, E. W., Padlan, E. A., Cohen, G. H., Smith-Gill, S. J., Finzel, B. C. & Davies, D. R. (1987) *Proc. Natl. Acad. Sci. USA* **84,** 8075–8079.
42. Bernstein, F. C., Koetzle, T. F., Williams, G. J. B., Jr., Meyer, E. F., Brice, M. D., Rodgers, J. R., Kennard, O., Shimanouchi, T. & Tasumi, M. (1977) *J. Mol. Biol.* **112,** 535–542.
43. Abola, E. E., Bernstein, F. C., Bryant, S. H., Koetzle, T. F. & Weng, J. (1987) In *Crystallographic Databases: Information Content, Software Systems, Scientific Applications*, eds. Allen, F. H., Bergerhoff, G. & Sievers, R. (Data Commission of the Int. Union of Crystallography, Bonn), pp. 107–132.
44. Amit, A. G., Mariuzza, R. A., Phillips, S. E. V. & Poljak, R. J. (1986) *Science* **233,** 747–753.
45. Colman, P. M., Laver, W. G., Varghese, J. N., Baker, A. T., Tulloch, P. A., Air, G. M. & Webster, R. G. (1987) *Nature (London)* **326,** 358–363.
46. Jeske, D., Milner, E. C. B., Leo, O., Moser, M., Marvel, J., Urbain, J. & Capra, J. D. (1986) *J. Immunol.* **136,** 2568–2574.
47. Sharon, J., Gefter, M. L., Manser, T. & Ptashne, M. (1986) *Proc. Natl. Acad. Sci. USA* **83,** 2628–2631.
48. Jeske, D. J., Jarvis, J., Milstein, C. & Capra, J. D. (1984) *J. Immunol.* **133,** 1090–1092.
49. Stevens, F. J., Chang, C. H. & Schiffer, M. (1988) *Proc. Natl. Acad. Sci. USA* **85,** 6895–6899.